



# Dynamic process of the Wenjiagou rock landslide in Sichuan Province, China

Han Dong Liu<sup>1</sup> · Dong Dong Li<sup>1</sup> · Zhong Fu Wang<sup>1</sup>

Received: 7 February 2018 / Accepted: 25 April 2018 / Published online: 16 May 2018  
© Saudi Society for Geosciences 2018

## Abstract

A rock avalanche is a geological event that is always sudden, rapid and with a long run-out, and can result in large loss of lives and property. The Wenjiagou rock avalanche was a high-speed rock landslide caused by a strong earthquake, in Mianzhu, Sichuan Province, southwest China. In this study, we reproduce the movement and deposition processes of the sliding mass by numerical simulation. We analyze the effects of the friction coefficient of each slip surface and the strength of the parallel bonds and contact stiffness between particles on the dynamic process and deposit features using three-dimensional particle flow code (PFC3D). The simulation results agree with the field measurements when the friction coefficient is 0.2, parallel bond strength is 2 MPa, and contact stiffness is  $2 \times 10^8$  kN/m. The landslide lasted about 115 s from the initial movement to the final deposition at the exit of the valley. The maximum velocity of the sliding mass was 114 m/s.

**Keywords** Rock avalanche · Numerical simulation · Dynamic process · Effect analysis

## Introduction

In nature, very different and contrasting flows can exist, such as the dry avalanche over natural terrain (Patra et al. 2005) and pyroclastic density current (Capra et al. 2018). The former is very fast, while the latter is very slow. A rock avalanche is a geologic event of high speed, long run-out, extensive influence, and strong destructive force; it can cause serious loss of lives and property and considerable changes to the surface environment (Clague and Souther 1982; Evans et al. 2001; Lube et al. 2007; Orwin et al. 2004; Shaller 1991). In the high mountains of Wenchuan County, Sichuan Province, southwest China, many rockslides caused by the 2008 Sichuan earthquake turned into rock avalanches consisting of rock fragments after intense collision, posing a great threat to people

at the downstream end of the valleys (Huang et al. 2008; Su et al. 2010; Wang et al. 2012; Wu et al. 2010).

The Wenjiagou landslide (location 31° 33' 04.7"N, 104° 06' 58.5"E) at the left bank of the Mianyuan River in Qingping Country, Mianzhu City, Sichuan Province, southwest China, is regarded as a typical high-speed rock avalanche resulting from a strong earthquake. It is located 3.6 km from the Longmenshan Fault. Many studies on the mechanism of high-speed rock avalanches have been published. Huang (2010) and Wang et al. (2010) used data from a field study of the Wenjiagou rock avalanche to examine the various stages of the avalanche using statistical analysis of the structural characteristics of the fragment deposition. Chen et al. (2011) combined field investigation and remote sensing interpretation to study the elements influencing rock avalanches and found that the geomorphology of the rock avalanche is the main factor controlling its movement and accumulation, and that several collisions lead to rock fragmentation. Jiang (2011) presents the mechanism of the collapse of the rock mass by simulating the avalanche process triggered by an intensive earthquake using three-dimensional distinct element code (3DEC). Liang (2014) studied landslide characteristics by comparing data derived from remote sensing images before and after the event. Zhang and Yin (2013) studied the rock particles in the accumulation zone of the Wenjiagou rock avalanche by performing laboratory tests,

✉ Dong Dong Li  
741721553@qq.com

Han Dong Liu  
Liuhandong@ncwu.edu.cn

Zhong Fu Wang  
xfjtwzf@163.com

<sup>1</sup> Henan Key Laboratory of Geomechanics and Structure Engineering, North China University of Water Resources and Electric Power, Zhengzhou 450046, China

including ring shear testing. They found that a decrease in particle size led to the high-speed landslide and divided the process into three stages: rock damage caused by karst evolution, rock-mass collapse caused by the earthquake, and debris flow along the Wenjiagou valley.

The studies mentioned above provided mainly qualitative descriptions of the geological characteristics and high-speed mechanism of a rock avalanche. However, literature about the movement of the avalanche and the extent of its influence is seldom encountered. Therefore, in this study, we reproduce the dynamic process of the Wenjiagou rock avalanche from the initial movement to the deposition by analyzing the effects of the friction coefficient of the slip surface, the strength of the parallel bond between the particles, and the normal stiffness of the contact using a three-dimensional (3D) numerical simulation model.

## Geomorphology and geological characteristics

### Terrain and landforms

The landform of the Wenjiagou valley was shaped by tectonic erosion, low-steep cutting slopes, and gully terrain. The highest point of the study site is Dingzi precipice, located on the eastern ridge of the valley, with an elevation of 2402 m, and the lowest point is the surface of the Mianyuan River at the gate of the Wenjiagou gully, with an elevation of 883 m, forming a maximum relative difference of 1519 m. The Wenjiagou valley is about 3 km long, whose shape resembles the shape of the number of 7 lying along an east-to-west axis (Chen et al. 2011).

Before the landslide, the depth of the gully was about 30–50 m, with some deeper sections. The slope of the gully bed was generally between 150 and 180‰ and deeper than 300‰ at the source of the avalanche.

### Strata and lithology

The main strata exposed in the area of the Wenjiagou landslide are Cambrian and Devonian strata. The Devonian Guanwushan group covers the Cambrian Qingping group with an angular unconformity boundary located above the fault scarp. The Guanwushan group is distributed in the valley mainly above 1300 m; the source rock has a medium-sloping dip angle and NW inclination, accompanied by karst. The Qingping group is distributed mainly in the gully below 1300 m and is the main stratum within the Wenjiagou area, with an overall tendency of N-NW. The regional tectonics produced folded strata, small faults, and other structural features.

## Characteristics of the landslide

The Wenjiagou rock avalanche occurred after rock damage caused by a strong earthquake. According to witnesses at the exit of the valley, the destabilized slope was first thrown high in the air, then fell, and began to slide. It is discovered that several severe collisions occurred between the avalanche debris and the mountain slope which changed the flow direction, with the debris being thrown up in a blast-like scenario (Huang et al. 2008). Based on the literature which described the debris accumulation and rock fragmentation in the Wenjiagou valley, we determined that the sliding mass collided with the valley slopes three times (Fig. 1). The landslide domain is divided into two zones: the landslide source area and the migration and accumulation area (Fig. 2). The characteristics of each zone are depicted below (Huang 2010).

### The source zone

The source area of the landslide is at the top of the eastern slope of Wenjiagou valley. It is 960 m long, 450 m wide at the head, and 1080 m wide at the trailing edge. The landslide body is 25–35 m thick with a surface area of 0.69 million m<sup>2</sup> and a volume of 27.50 million m<sup>3</sup>. This area is trapezoid shaped with the lower part covered by an inverted rock cone lying NNE-SSW. The base of the landslide body is grayish white limestone and dolomitic limestone which is moderately weathered, with an orientation of 320°∠32°. The rock of the source area is hard, with a clear sound heard and obvious rebound after hammering. Two controlled scarps can be seen clearly on the back wall after the slide (Fig. 3).

### Analysis of the landslide dynamics and deposit process

The rock mass at the top of the Wenjiagou valley became unstable and slid over a weak structural plane after the strong earthquake. The rock mass slid about 690 m, then collided with the opposite side of the valley at the Hanjia plane, and proceeded to slide off the cliff in the direction 290°. Because of the violent collision, the sliding rocks melted and the liquidized rock changed direction to 230°, flowing into the main accumulation zone. After flowing for 730 m in the valley, a second collision occurred, with the southern slope of the Wenjiagou valley, resulting in another turn where the landslide moved 180 m in the direction 310° before colliding with the northern slope of the valley.

After the third collision, the debris avalanche moved directly to the valley exit; then, a collapse area 400 m long and up to 50 m wide appeared, caused by the erosion at the southern part of the valley by the low-viscosity debris. A light collision and another change in the flow direction occurred in the deposit zone as a result of the topography, but this effect was smaller

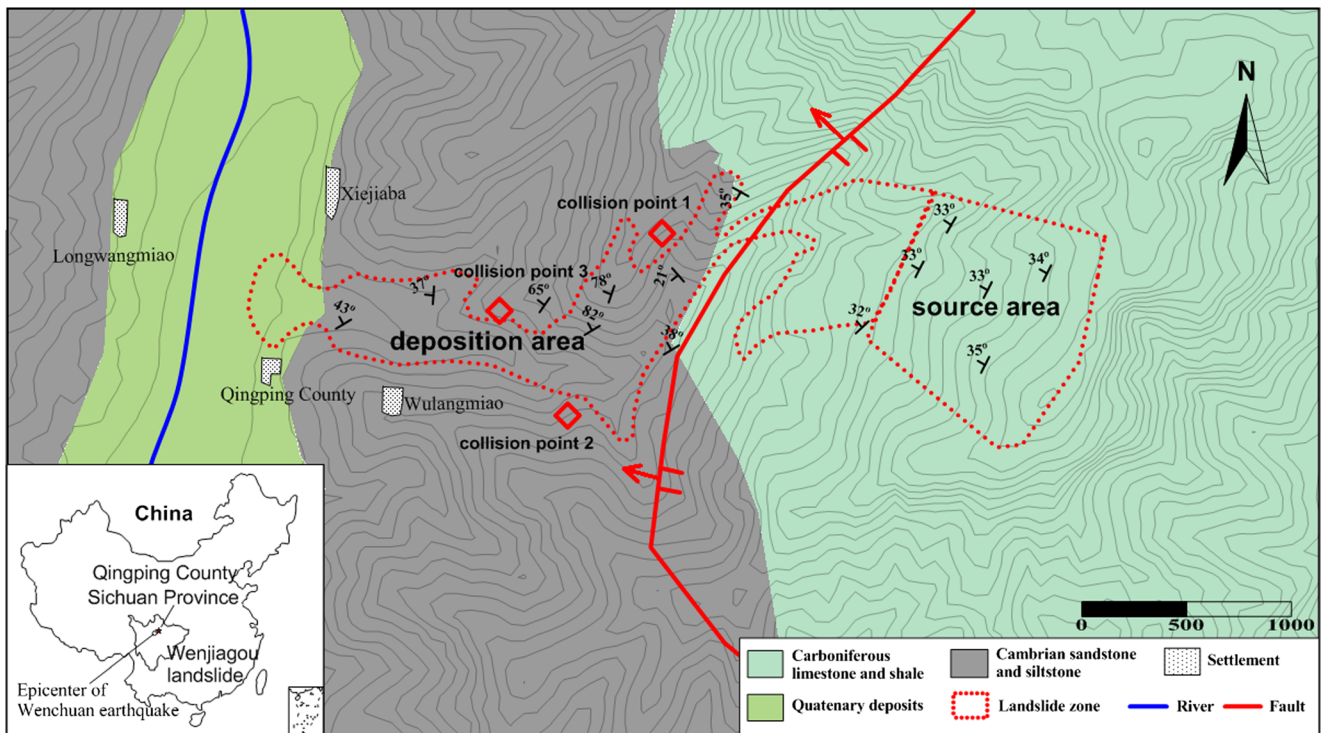


Fig. 1 Geologic map of the Wenjiagou rock landslide zonation

than the three previous events. Most of the debris continued to move for 420 m at 266° before coming to rest.

## Numerical simulation

### Conception of the PFC3D

Particle flow code (PFC) is a commercial software for the simulation of media mechanism developed by ITASCA based on the discrete element method (DEM) (Cundall and Strack 1979; Potyondy and Cundall 2004). The technique is used to

simulate the cracking process and large displacement of granular assemblies and the flow of particles from the microscopic point of view. PFC can effectively simulate the deformation and flow of cementing materials and the damage and fracture process of an elastic brittle medium. Utilizing the explicit calculation principle of DEM, the contact force of ball-ball and wall-ball is derived based on the principle of force displacement (Eqs. 1, 2, and 3) (Larson et al. 1998; Su and Akcin 2011).

$$F_i = F_i^n + F_i^s \tag{1}$$

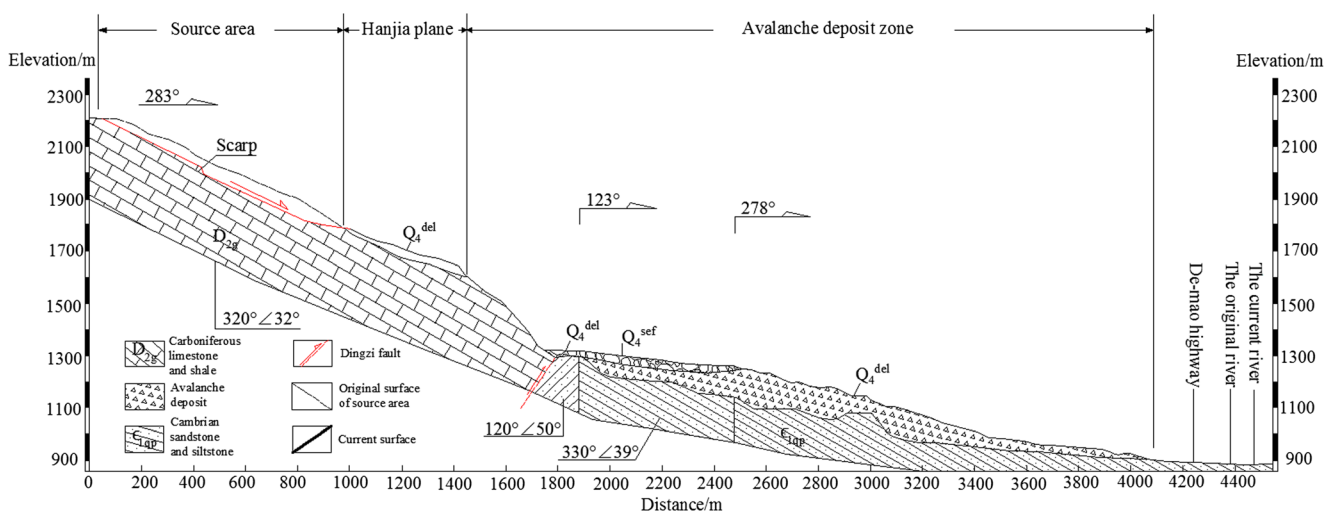


Fig. 2 Longitudinal geological cross section of the Wenjiagou rock landslide (Huang 2010)

**Fig. 3** The source area of the Wenjiagou rock landslide (Zhang et al. 2016)



$$F_i^n = K^n U^n n_i \quad (2)$$

$$\Delta F_i^s = -k^s \Delta U_i^s \quad (3)$$

where  $F_i$  is the contact force (which represents the action of ball A on ball B for ball-ball contact, and the action of the ball on the wall for ball-wall contact);  $F_i^n$  and  $F_i^s$  denote the normal and shear component vectors, respectively;  $K^n$  is the normal stiffness at the contact;  $U^n$  is defined to be the relative contact displacement in the normal direction;  $n_i$  means the contact plane; and  $\Delta U_i^s$  is the shear component of the contact displacement-increment vector, which is used to calculate the shear elastic force-increment vector ( $\Delta F_i^s$ ) with the shear stiffness ( $k_s$ ) at the contact.

The velocity and up-to-date position of each particle are achieved from the Newton's second law of motion (Eq. 4).

$$F_i = m(\ddot{x}_i - g_i) \quad (4)$$

where  $m$  is the total mass of the particle,  $\ddot{x}_i$  is the acceleration, and  $g_i$  is the body force acceleration vector (e.g., gravity loading).

As a discrete element model, PFC has some advantages in modeling landslides which were controlled by structural planes and can occurred significant disintegration during the course of movement. The PFC model does not limit the scale of separation and displacement behaviors of elements, and the movement process of the mass from fracture to separation can be fully simulated. What is more, the model has been used to simulate several real landslides cases (Tang et al. 2009; Lo et al. 2011; Lu et al. 2014). Depending on the characteristics and wide use, PFC was chosen for the modeling. We analyzed the effects of the friction coefficient, contact stiffness, and the particles' parallel bond strength on the velocity, displacement, and final distribution of the debris. Moreover, the debris characteristics were obtained by monitoring the number of parallel bond contacts and obtaining the bond breakage number of the sliding event.

## Parameters

To simulate the energy dissipation process of the landslide, mechanical damping is introduced into the numerical model, which includes local damping and viscosity damping. While the former is realized by adding a damping coefficient to the equation of motion, the latter is modeled as the energy loss in the contact process (Cundall and Strack 1979). Extensive testing has shown that for the same damping coefficient, the degree of energy dissipation is related to the number of particles; the more particles there are, the more contact and more dissipation occur. The parameter of damping in PFC affects the motion of particles and energy dissipation during collision. Local damping applies a damping force, with magnitude proportional to unbalanced force, to each ball. Viscous damping adds normal and shear dashpots at each contact. For problems involving free flight of particles and/or impacts between particles, local damping is inappropriate, and viscous contact damping should be used. While this parameter is not explicitly related to any physical mechanism, the viscous contact damping coefficients of Wenjiagou rock landslide are estimated based on previous studies (Tang et al. 2009; Lo et al. 2011; Lu et al. 2014; Lin and Lin 2015), considering the relationship between the critical damping ratio and the restitution coefficient, and the results of restitution coefficient tests in the field by Giani (1992).

The parameters reflecting the microscopic characteristics of the rock material should be determined when we conduct numerical computation with PFC3D, unlike simulation of continuum medium. The matching of microscopic and macroscopic parameters is achieved by conducting numerical triaxial tests (Lo et al. 2011; Potyondy and Cundall 2004).

The macroscopic parameters used in our analysis are the uniaxial compressive strength (UCS), Young's modulus ( $E$ ), and Poisson's ratio ( $\mu$ ), while the microscopic parameters include the minimum radius ( $R_{\min}$ ), particle diameter ratio ( $R_{\max}/R_{\min}$ ), contact modulus ( $E_c$ ), particle stiffness ratio ( $k_n/k_s$ ), particle friction coefficient ( $f$ ), parallel bond radius

multiplier ( $\lambda$ ), ratio of parallel bond modulus ( $k_n/k_s$ ), normal strength of parallel bond ( $pb\_nstr$ ), and the shear strength of the parallel bond ( $pb\_sstr$ ).

The relationship between the macroscopic modulus and microscopic parameters is defined by Eq. 5:

$$E_c = \frac{k_n}{4R}, \underline{E}_c = k_n (R^{(A)} + R^{(B)}) \quad (5)$$

where  $k_n$  is the normal stiffness of the particle,  $R$  is the particle radius,  $\underline{E}_c$  is the parallel bond modulus,  $k_n$  is the contact stiffness of parallel bond, and  $R^{(A)}$  and  $R^{(B)}$  are the radius of two particles (named A and B) attached by parallel bond. The Poisson's ratio is related to the stiffness and geometry of the accumulation area; the peak strength is based on the friction coefficient and bond strength.

The microscopic parameters for the simulation of the Wenjiagou rock avalanche were determined by simulating a uniaxial compressive test and comparing the results (UCS, Young's modulus, and Poisson's ratio) with those obtained in a laboratory experiment. The sample used in the simulation of the uniaxial compressive test is 4 m high, 2 m in diameter (height/diameter ratio of 2), and is made of 2145 spheres. The UCS, Young's modulus, and Poisson's ratio were derived by a strain-controlled uniaxial test.

By conducting many numerical simulations of the uniaxial compressive test, the microscopic parameters representing the mechanical properties of the source rock were derived (Table 1). Comparison between the simulation tests and mechanical parameters of the limestone in the Wenjiagou landslide found in the literature is presented in Table 2. The simulation results were close to those of the laboratory experiments, confirming that the microscopic parameters can be used to simulate the dynamic process of the landslide mass before the rock underwent fragmentation.

**Table 1** The numerical parameters of the PFC modeling

Parameters	Parameter values used in modeling
Density (kg/m <sup>3</sup> )	2720
Normal stiffness (N/m)	2e8
Shear stiffness (N/m)	2e8
Friction coefficient	0.35
Normal strength of contact bond (Pa)	1.0e6
Shear strength of contact bond (Pa)	1.0e6
Normal stiffness of parallel bonds (N/m <sup>3</sup> )	1.6e10
Shear stiffness of parallel bonds (N/m <sup>3</sup> )	1.6e10
Radius of parallel bonds (m)	0.5
Normal strength of parallel bonds (Pa)	2.0e7
Shear strength of parallel bonds (Pa)	2.0e7

**Table 2** Parameter values of rock samples determined by laboratory and numerical simulations

Item	Limestone	Numerical sample
Density (kg/m <sup>3</sup> )	2720	2720
Young modulus (GPa)	71.70	72.24
Poisson's ratio	0.21	0.20
Uniaxial compressive strength (MPa)	168.00	171.07

## Numerical model

The sliding surface is divided into three parts by two scarps which can be seen clearly on the satellite photograph. This suggests that the sliding mass did not start moving as one unit but was divided into three parts, as shown in Fig. 5. Therefore, for our simulation, we defined the three zones, area I, II, and III, as the conditions at the start of the landslide. This initial condition has a strong effect on the process of rock fracture, movement, and accumulation during the landslide. Region I has an area of 172,000 m<sup>2</sup>, area II is 269,000 m<sup>2</sup>, and area III is 155,000 m<sup>2</sup>. The sliding mass consists of 12,500 particles, with a total volume of 23 million m<sup>3</sup>.

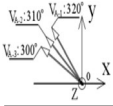
The sliding surface of the collapse area of the Wenjiagou rock avalanche model is constructed with 13,146 wall elements based on a 30 × 30-m DEM created after the event. The deposit area was determined based on a previous field survey (Huang et al. 2008). The total length of the sliding surface from east to west is 5875 m; the total width from north to south is 3250 m.

## Initial and boundary conditions

According to Huang et al. (2008) and Shi (2014), the three parts of the sliding mass started moving one by one with a time interval of 5 s. This paper mainly focuses on the movement and deposition process of the Wenjiagou rock landslide. The initial velocity of sliding mass was achieved by characteristic parameters of seismic waves, recorded by Qingping seismic station nearest to the Wenjiagou rock landslide, considering that the amplification effect of amplitude occurs at the top of the mountain (Shi 2014). The velocity and velocity components are shown in Table 3.

A 3D surface represents the boundary of the movement of the rock avalanche. However, because of the difference between the soil and rock parameters and the vegetation distribution, the friction coefficient of the sliding surface changes depending on the position. Some phenomena in the landslide process are difficult to reproduce in PFC3D; these include the fluidization characteristic caused by the mixing of the sliding mass and air and the erosion of the side and bottom of the valley (as demonstrated by the volume change of the sliding mass before and after the event). Hence, in our model, the 3D

**Table 3** Original velocity of the source rock of the Wenjiagou landslide (Shi 2014)

Original velocity and the direction	Part	Total time (s)	Velocity (m/s)	Component of velocity(m/s)		
				$V_x$	$V_y$	$V_z$
	I	5	0.30	-0.15	0.18	-0.18
	II	10	0.42	-0.26	0.22	-0.26
	III	15	0.52	-0.36	0.21	-0.31

surface is simplified and the friction coefficient is assumed to be constant during the movement of the landslide body.

### Layout of monitoring points

As our study aims to understand the landslide mechanism of high velocity and long run-out by numerical simulation, it is significant to record the velocity, displacement, energy change, and trajectory of each part of the sliding body during the movement process. As the three parts of the sliding mass started moving at different times, they are monitored separately, with 15 monitoring points in part I, 16 points in part II, and 25 points in part III (Fig. 4). Six representative profile lines (I-I', II-II', III-III', IV-IV', V-V', VI-VI') are presented in Fig. 5.

### Numerical simulation results

The velocity and deposition characteristics of a rock avalanche are affected by various factors. The velocity is closely related to the friction characteristics of the slip

surface, while the run-out and area of deposition is also related to the geomorphology and distribution of obstacles along the sliding path. The friction coefficient varies depending on the materials of which the slope is comprised; therefore, it is not a constant value. To determine a value reflecting the overall friction characteristics of the slip surface, four values of friction coefficient (0.1, 0.2, 0.3, and 0.4) were chosen to study their effects on the patterns of movement and deposition. The strength of the particle bond is related to the uniaxial compressive strength, while according to Hoek and Brown (1997), the compressive strength of the field rock material is lower than that obtained in laboratory tests. Thus, the effects of three values of parallel bond strength (0, 2, and 20 MPa) were explored too. Moreover, three values of contact stiffness ( $2 \times 10^7$ ,  $2 \times 10^8$ , and  $2 \times 10^9$  kN/m) were adopted to study the effects of collision on the movement and accumulation characteristics. Table 4 shows the run-out distance and falling height of the debris mass under various mechanical parameters as well as the field measurements obtained by Huang (2010).

**Fig. 4** Position of monitoring points on the surface of the source area

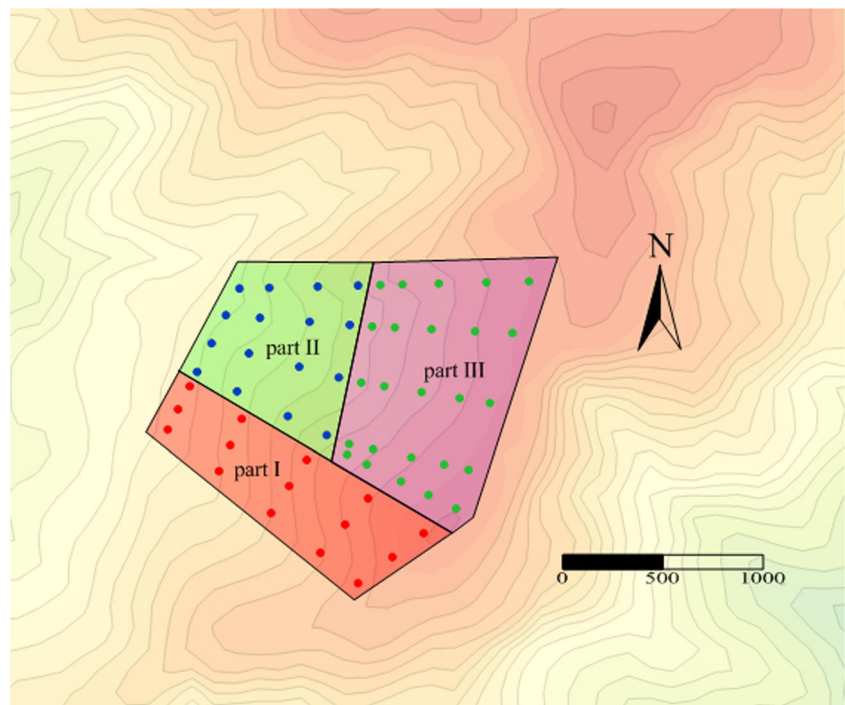
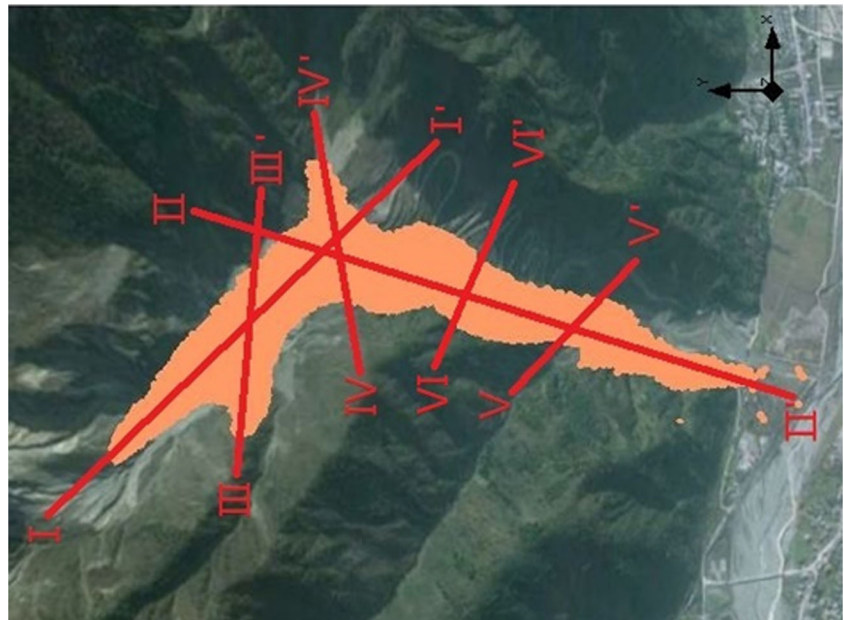


**Fig. 5** Position of the six typical profiles across the landslide path



### Effect of the friction coefficient of the slip surface

Figure 6 shows the debris deposition area and shape under different values of friction coefficient, with the vertical profiles shown in Fig. 7. While most of the debris mass was deposited in the Wenjiagou valley, from the bottom of the escarpment under the Hanjia plane to the valley exit, some of the material flowed across the Mianyuan River. The different flow patterns demonstrate the strong effect of the friction coefficient of the slip surface. The run-out distance and width of the tailing edge decrease as the friction coefficient increases. When the friction coefficient is 0.1, large amounts of debris mass slide across the Mianyuan

River to the opposite bank; this flow pattern differs from survey results that most of the debris mass stopped at the exit of the valley (Huang et al. 2008). With a friction coefficient equal to 0.2, the position of the leading and tailing edges and the width of the debris deposition agree with those of the field investigation. For friction coefficients of 0.3 and 0.4, the run-out distance is smaller than that measured in the field. Therefore, the friction coefficient of 0.2 was the best fit one.

### Effect of the strength of the parallel bond between particles

Figure 8 shows the effect of the parallel bond strength on the movement characteristics and deposit pattern of the landslide mass, and the vertical profiles are presented in Fig. 9. The influence of the parallel bond is not as apparent as that of the friction coefficient. As the parallel bond becomes stronger, the run-out distance decreases, with most of the debris mass deposited in the valley and some sliding into the tributary of the Wenjiagou valley. The debris mass has a farthest run-out distance (4240 m) when the parallel bond strength is zero; this distance is considerably further than that measured in the field. This indicates that the debris particles undergo fluidization which lowers or eliminates their cohesion, leading to a longer run-out distance. The distribution and position of the deposition mass are similar to the field survey results when a parallel bond strength of 2 MPa is used, yielding a run-out distance of 4168 m. When the parallel bond

**Table 4** Run-out distance and fall height for different parameters

Sorts of parameters		Run-out distance (m)	Falling height (m)
Friction coefficients	0.1	4547	1473
	0.2	4175	1362
	0.3	3708	1346
	0.4	3634	1341
Strength of parallel bond (MPa)	0	4240	1368
	2	4168	1361
	20	4082	1357
Contact stiffness (kN/m)	2e7	4125	1380
	2e8	4167	1363
	2e9	4193	1352
Investigate results by Huangheqing		4170	1360

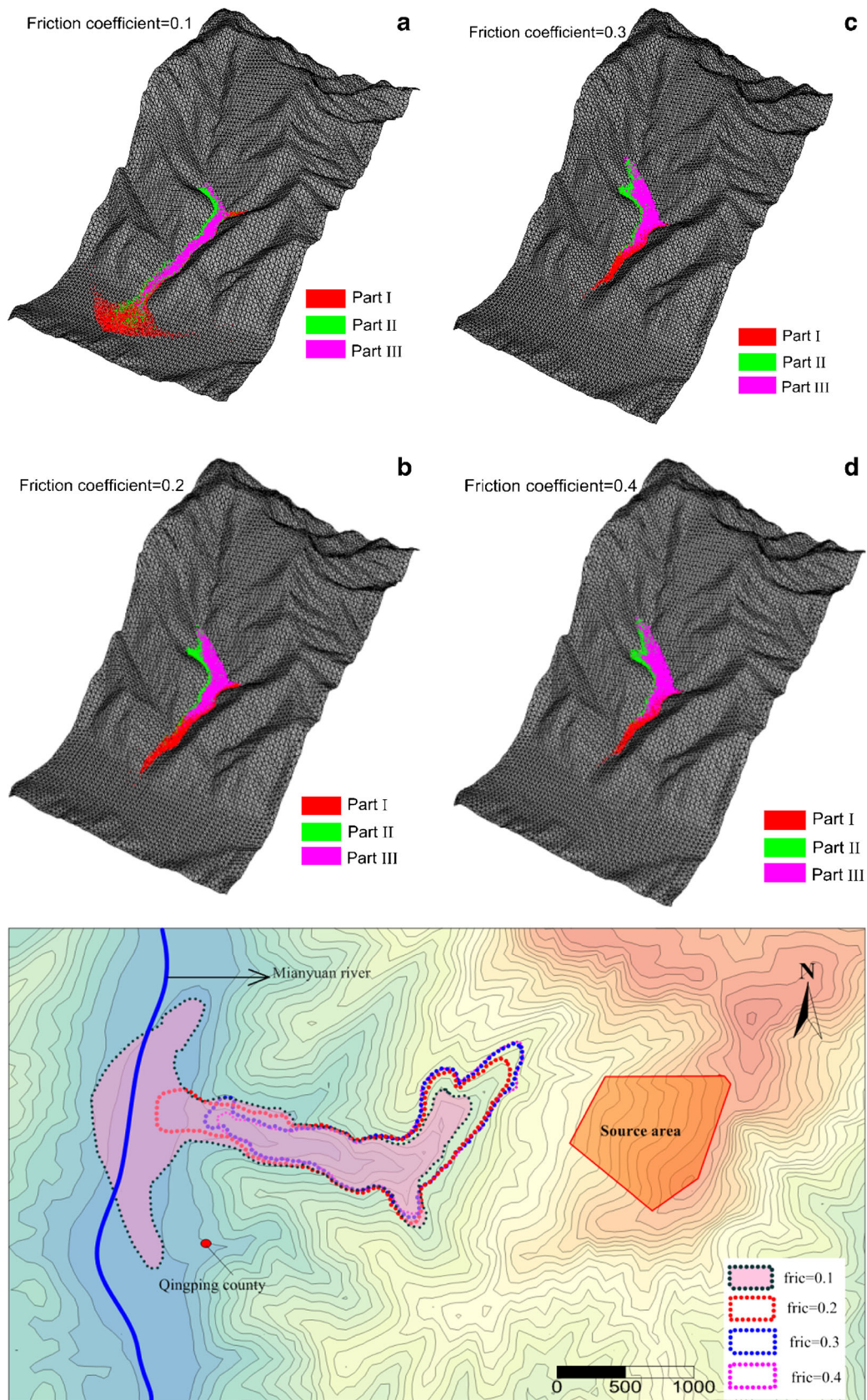


**Fig. 6** Effect of friction coefficient on the deposit pattern and area of the debris mass. **a–d** 3-D models. *bottom* Topographic area map



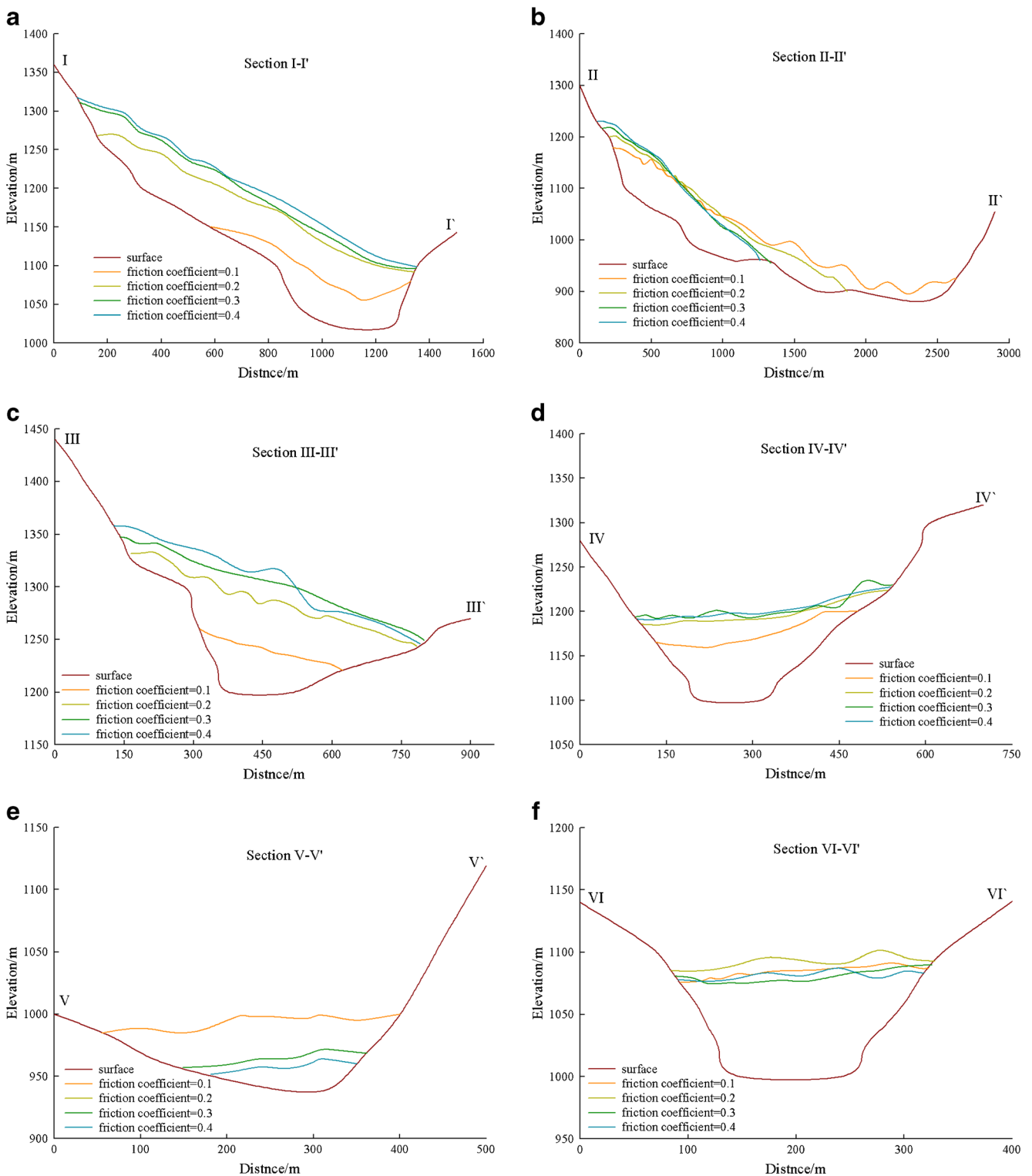


**Fig. 7** Typical vertical profiles of deposit mass for four friction coefficient values along the six profile lines (shown in Fig. 5)

strength is 20 MPa, the rock mass does not break easily and the fluidity is limited; therefore, the run-out is less than the actual value. For the three parallel-bond strength values tested in our model, 2 MPa was more reasonable than the others.

**Effect of the contact stiffness**

Figure 10 shows the effect of the contact stiffness on the run-out and deposit pattern; comparison of six different sections was presented in Fig. 11. As the contact stiffness increases, the

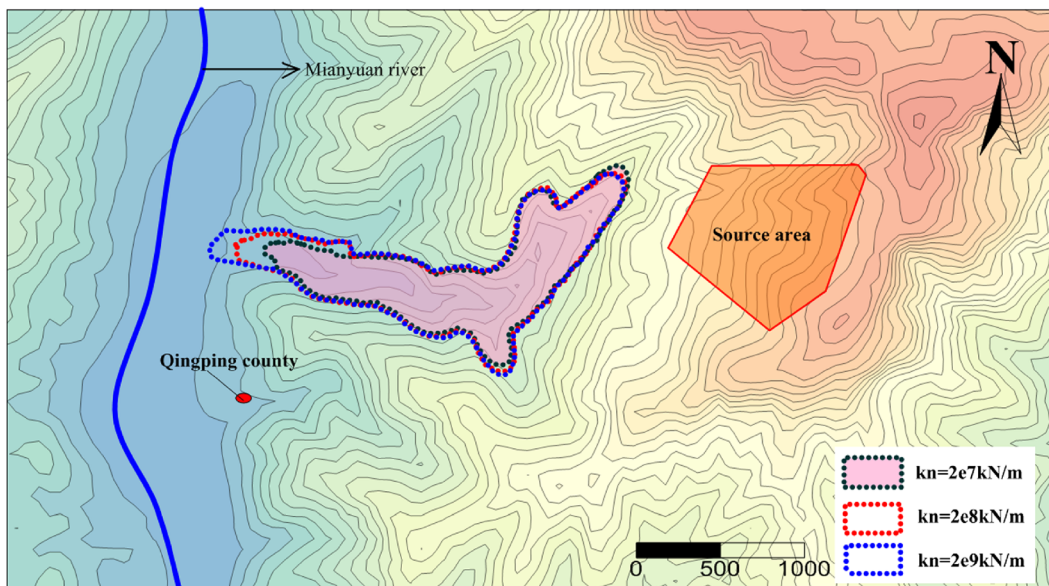
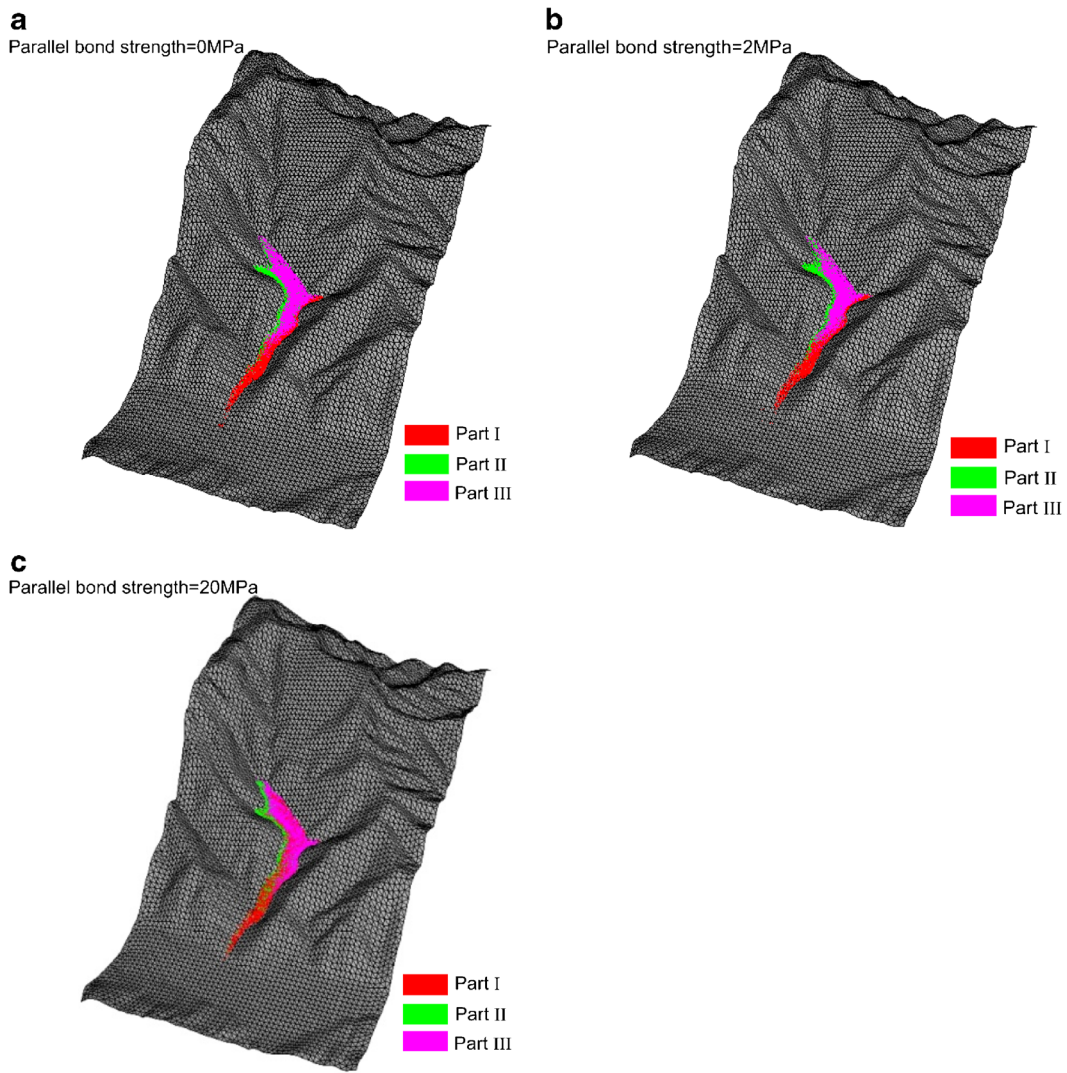


**Fig. 8** Effect of parallel bond strength on landslide deposit pattern and area. **a–c** 3-D models. *bottom* Topographic map

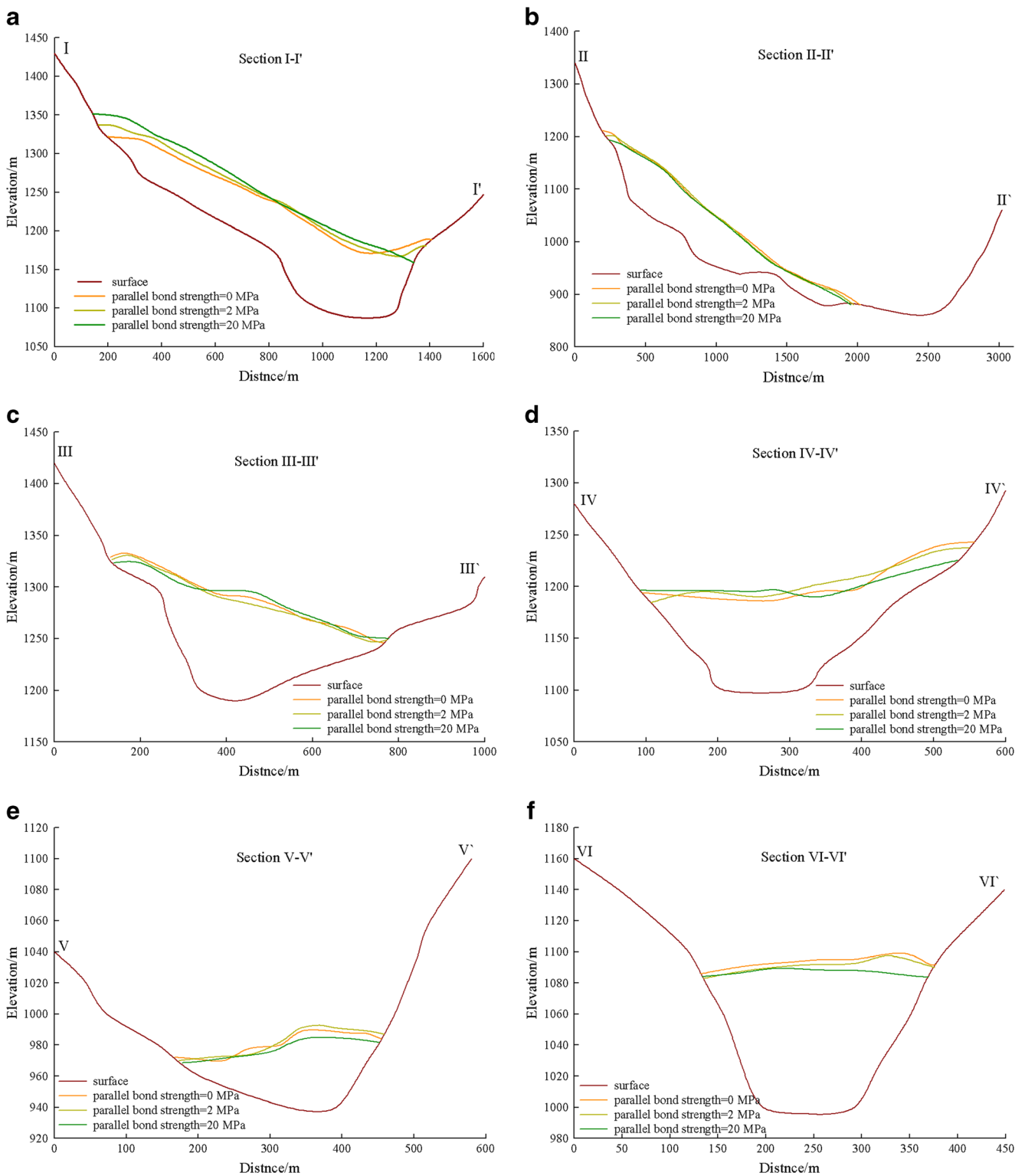


**Fig. 9** Typical vertical profiles of the deposit mass for three parallel bond strength values along the six profile lines (shown in Fig. 5)

run-out distance increases, as well as the degree of accumulation. The effect of contact stiffness on run-out is greater than that of parallel bond strength. The longer run-out distance may be due to the increment of energy passed from one particle to

another as the contact stiffness increases. As was shown in Fig. 10, most of the debris mass deposited in the main valley; only minor part of it slid into the tributary of the valley. The run-out distance and area of deposit closest to the field

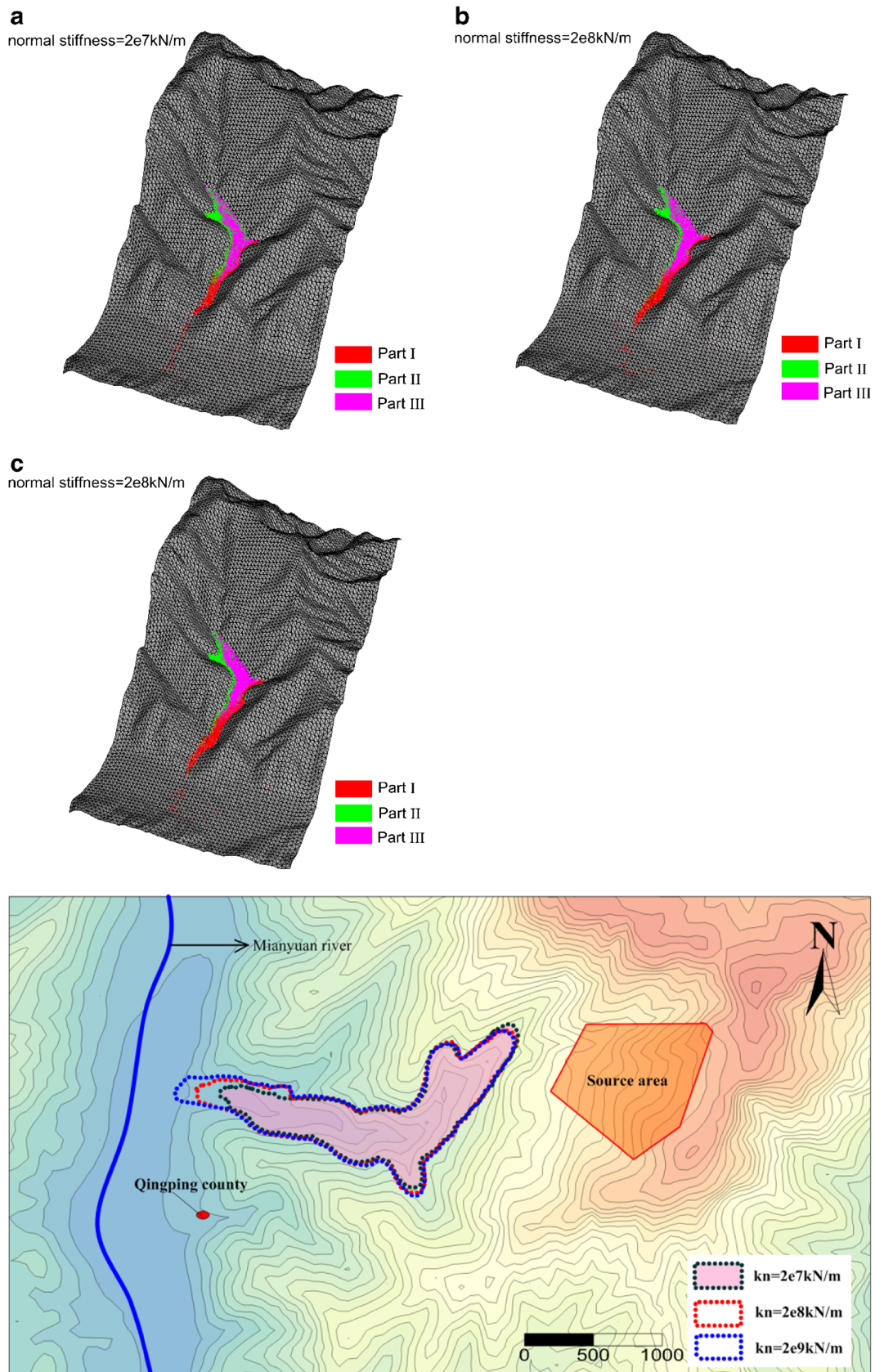
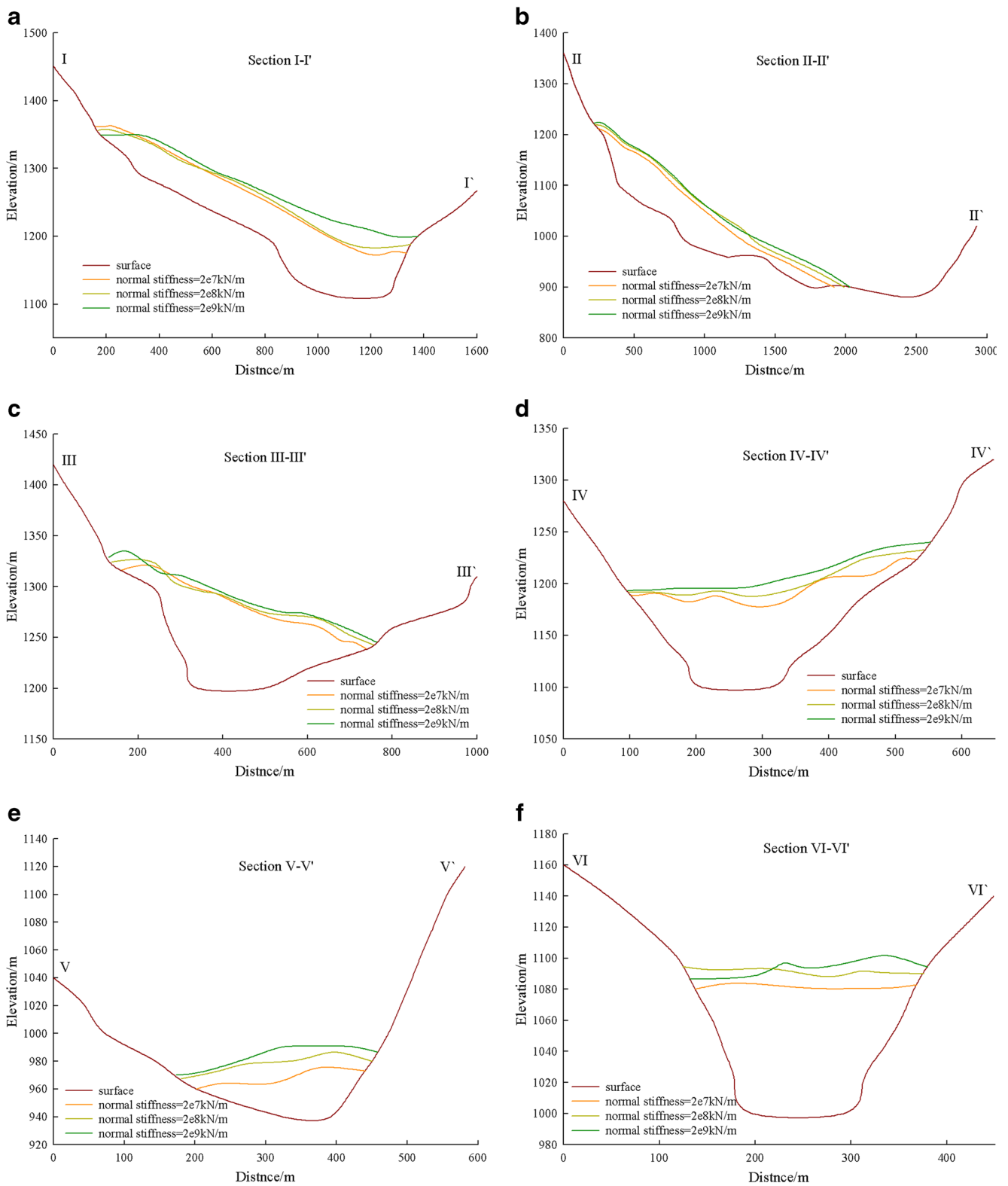


Fig. 10 Effect of contact stiffness on deposit pattern and area of the landfill mass. **a–c** 3-D models. *bottom* Topographic area map



**Fig. 11** Typical vertical profiles of the deposit mass for three contact stiffness values along the six profile lines (shown in Fig. 5)

measurements were achieved with a contact stiffness of  $2 \times 10^8$  kN/m; the next best fit was for a contact

stiffness of  $2 \times 10^8$  kN/m, followed by  $2 \times 10^9$  kN/m, and finally  $2 \times 10^7$  kN/m.

## Analysis of the dynamic process of the landslide

The analysis of the effect of the various parameters presented in the “Numerical simulation results” section and comparison with the field measurements show a good fit between the simulation results and the actual values for a friction coefficient of 0.2, parallel bond strength of 2 MPa, and contact stiffness of  $2 \times 10^8$  kN/m. To illustrate the dynamic process of the rock avalanche, the position of the sliding mass, velocity of every particle, velocity history of the monitoring points, and the broken parallel bonds were recorded. The simulation results of the dynamic process of the Wenjiagou rock avalanche are presented below.

### Dynamic process of the sliding mass

Figure 12 illustrates the position of the sliding mass at different times. The initial position of the three regions (parts I, II, and III) is shown in Fig. 5. The position of the three parts after 5, 10, and 15 s is shown in Fig. 12a–c, respectively, during which the sliding mass slides along the slip surface, maintaining its original shape. Part I and part II reach the Hanjia plane at 15 s, and collide with the mountain opposite the plane at 30 s, whereby the colliding mass becomes fragmented and fluid. This agrees with Fig. 15, which shows that most of the parallel bonds are broken at this stage. After the collision, the sliding direction of the landslide changes from  $290^\circ$  to  $230^\circ$ . Then, between 30 and 40 s, the sliding mass collides with the south bank of the valley, leading to partial energy dissipation and local deposition. As the sliding mass continues to move down the valley, it encounters the narrowing landform, colliding repeatedly with both sides of the mountain, which absorb much more energy. Eventually, the debris of the rear edge of the sliding mass stops at 70 s and most of the debris mass finally comes to rest at 115 s.

### Velocity distribution of the sliding mass

The velocity contour of the sliding mass at different times is shown in Fig. 13, and the velocity of the monitoring points with time along the axial directions is shown in Fig. 14. The sliding mass reached the maximum velocity (114 m/s) between 30 and 40 s, when the landslide slid off the Hanjia plane to the opposite mountainside. After 5 s, the leading edge of part I of the landslide, which moved first, reached a velocity of 37–49 m/s, partially arriving at the Hanjia plane. Five seconds after part II began to slide, it reached a maximum velocity of 43–58 m/s. Then, the velocity increased to 57–75 m/s, 5 s after part III started sliding, forming a high-velocity base for the sliding mass which ruptured from the mountain, creating the upper scarp between 15 and 30 s, with a maximum velocity of 106 m/s. After the sliding mass collided with the mountain

opposite the Hanjia plane, the sliding direction changed and some of the debris was deposited. At 30–40 s, the sliding mass collided with the south side of the valley, leading to a decrease in the velocity, while the rear edge of the landslide with high acceleration reached the peak velocity of 114 m/s. Because of the two collisions, the velocity and energy levels of the moving mass decreased gradually. The velocity of the rear part of the landslide decreased to 5 m/s at 70 s; then, most of the particles settled in the deposition area as the velocity decreased to 0 m/s.

As shown in Fig. 14, the maximum velocity in the *X* direction is 45–50 m/s for part I, 35–40 m/s for part II, and 50–55 m/s for part III. In the first 20 s, the velocity in the *X* direction increased gradually; then, at 20–30 s, it decreased until the collision with the mountain at about 30 s, which caused an increase in the velocity. Because of the energy dissipation and lower velocity resulting from the collision with the mountain, some of the sliding mass was deposited as it moved ahead. Most of the particles of part I stopped moving at about 115 s, those of part II at about 100 s, and those of part III at about 90 s, as the velocity decreased to zero.

The *Y* direction is close to the main sliding direction. In the *Y* direction, there are three notable velocity changes caused by three collisions with the valley slopes, which is more notable than that of part II and part III. The peak velocity appeared at 30–40 s and was 75–80 m/s for part I, 65–70 m/s for part II, and 80–85 m/s for part III. In the *Z* direction, the particles were strongly bound because of the severe collision forces. The peak velocities for parts I, II, and III were 75–80, 60–65, and 75–80 m/s in the *Z* positive direction, respectively, and 45–50, 25–30, and 10–15 m/s in the negative *Z* direction, respectively.

### Disintegration of the sliding mass

The breakup process of the sliding mass during its movement can be reflected by the number of broken parallel bonds. Most of the parallel bonds broke during the initial 20 s (Fig. 15), indicating that the main sliding mass entirely collapsed and fragmented into debris during that time.

## Discussion

### Evaluation of the kinematic process modeling

In order to simulate the kinematic process of the rock landslide successfully, the numerical model should meet constraints from eyewitness and field investigation. Some agreements such as the volume, the position of the source area, and the terrain of the sliding surface were obeyed in this case. However, the selection of the friction coefficient of the sliding surface, the parallel bond strength, and the contact stiffness were made as indirect

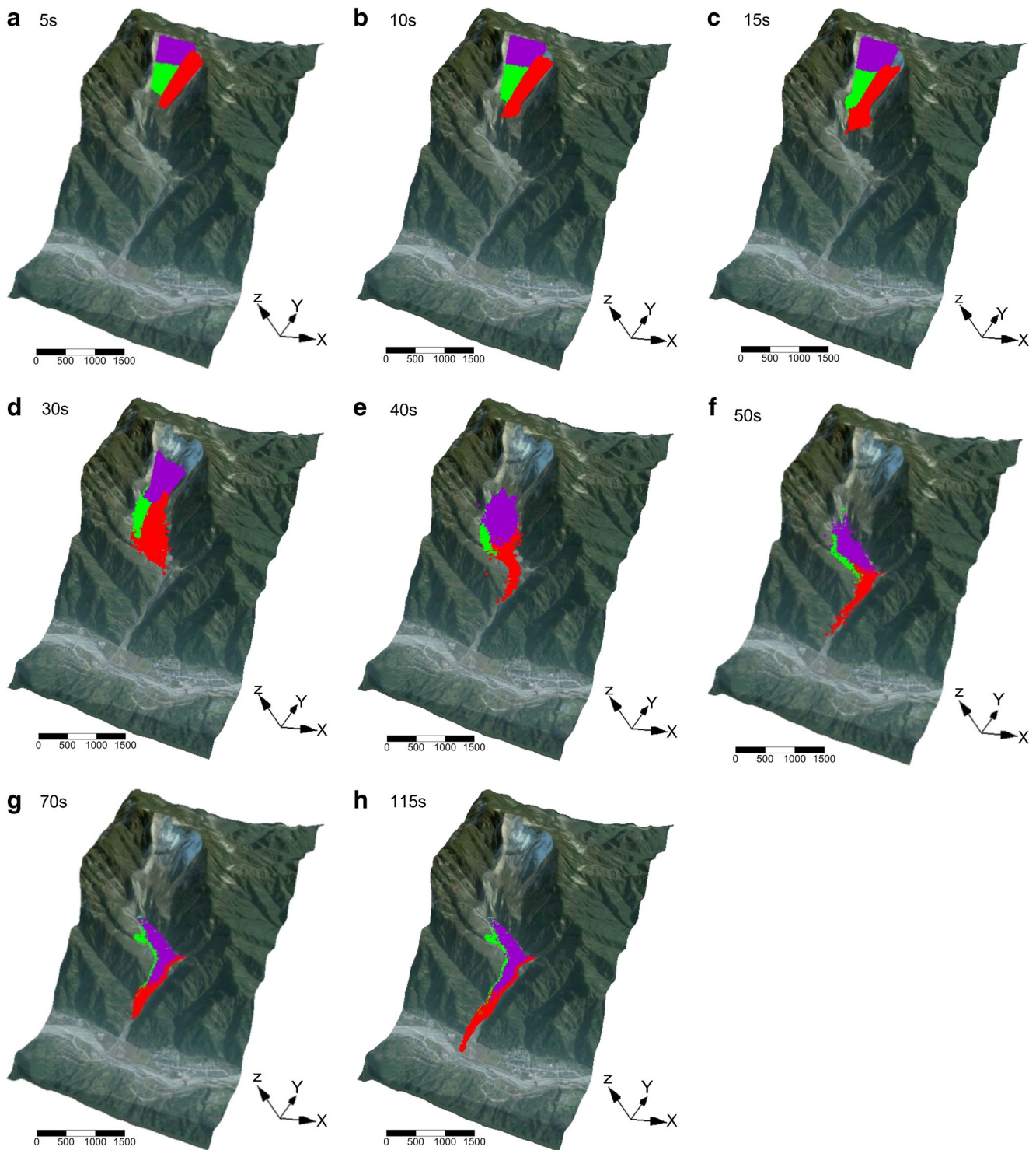


**Fig. 12** Movement process of the Wenjiagou rock avalanche: region I—red, region II—green, and region III—purple

factors to meet the known deposition characteristics. According to the numerical simulation results, most of the particles finally deposited in the Wenjiagou valley forming the landslide dam, and the final deposition pattern agrees well with field investigation by Huang

(2010). Besides, changes of the particle velocity along the kinematic process were in accordance with the transition from the steep source area to the gentle slope in the downstream of the valley, and the collision between the sliding mass and the mountain.

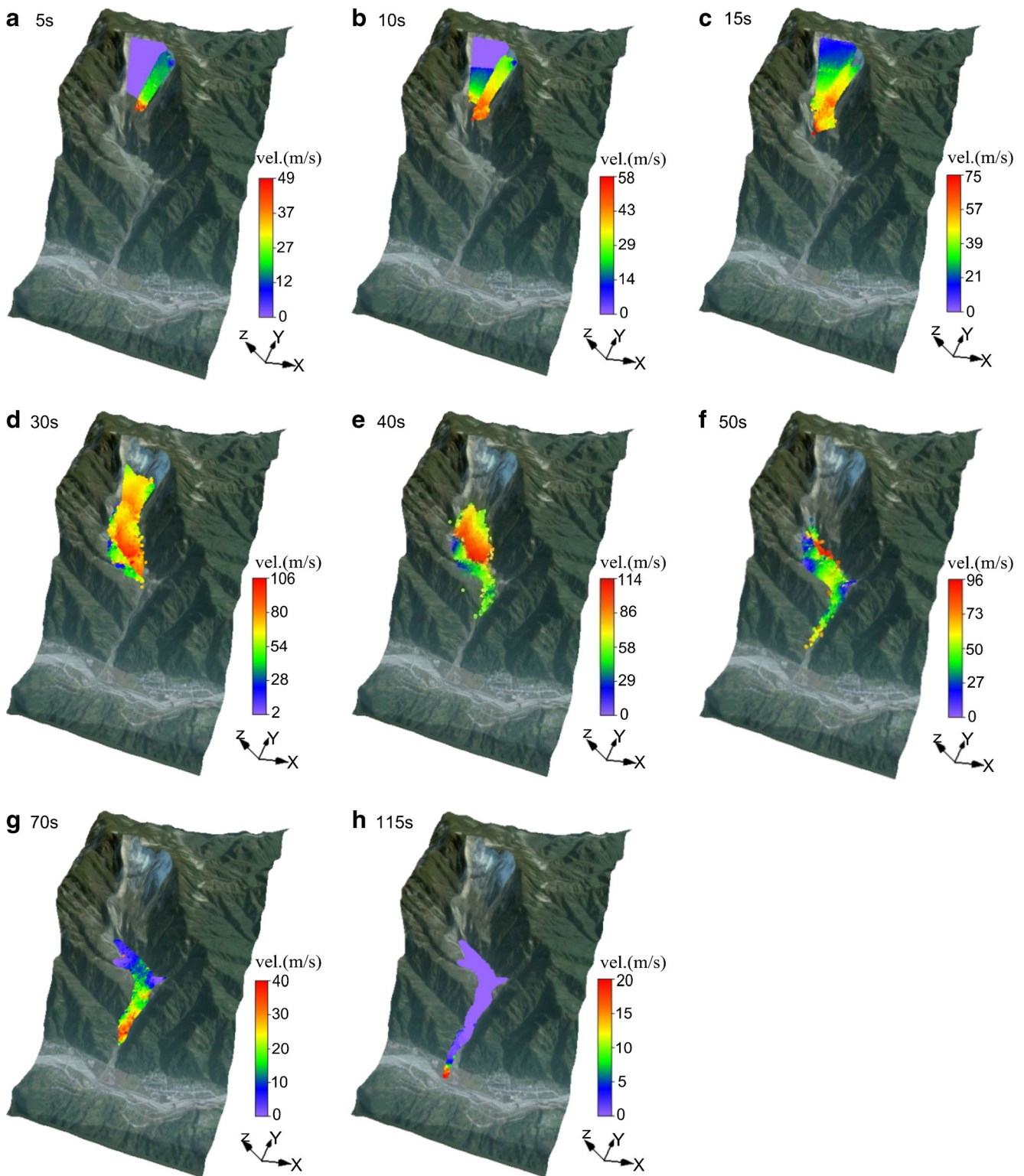


Fig. 13 Velocity contours at different times; units in m/s

### Limitations of the PFC model

There are some limitations of the PFC3D models and perspectives for the scenario simulations of other potentially

catastrophic landslides. Firstly, number of the particle element is generally not sufficient to simulate the failure mechanism in detail. Diameter of particles may be too large in diameter to simulate exactly the potential landslide-affected area and



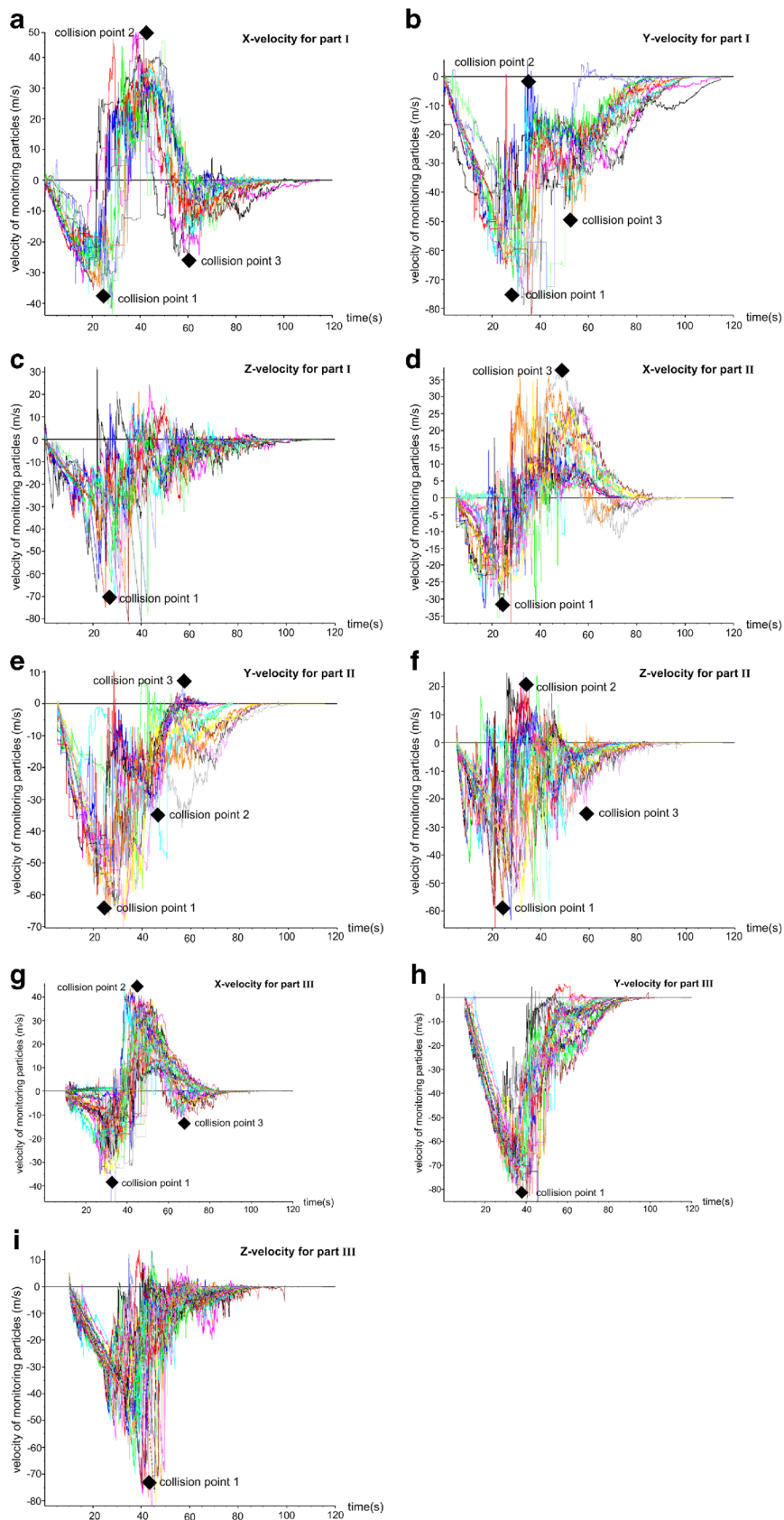
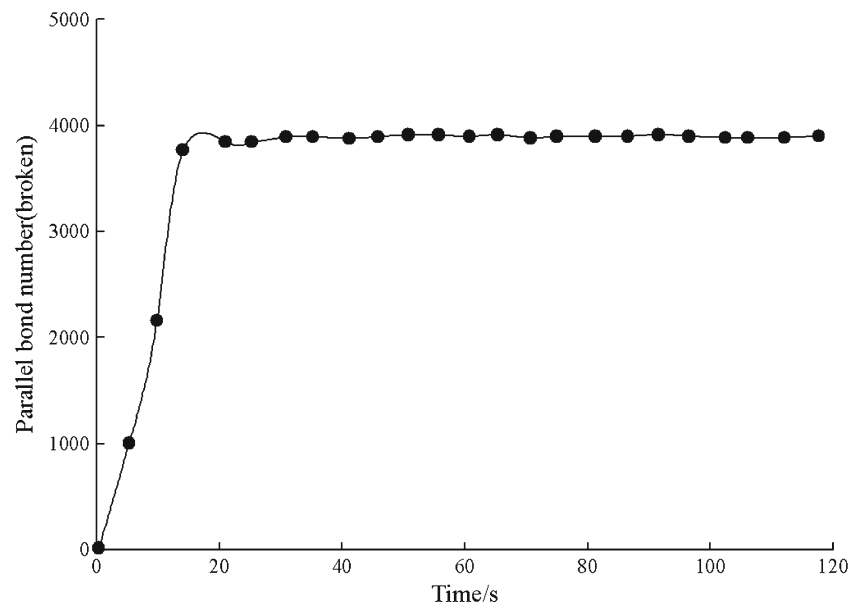


Fig. 14 Plots of velocity (m/s) vs. time (s) recorded at the monitoring points for the X, Y, and Z directions

**Fig. 15** Number of broken parallel bonds vs. time



reliably represent rock shape. Secondly, the slip surfaces were considered to be rigid without deformation. However, the sliding mass may take some accumulation away along the valley in reality. Because of the limitations of the PFC3D model, it was hard to simulate the erosion of slide bed resulting from the movement of sliding mass. Thirdly, friction coefficient of each slip surface was set to the same value due to the difficulty of making friction coefficient changing depending on the type of material. According to the numerical simulation results shown in Fig. 12, the kinematic process of the sliding mass was achieved using an integrative friction coefficient.

## Conclusions

In this article, the basic characteristics of the Wenjiagou rock avalanche are depicted and analyzed. Then, the particle flow code PFC3D is used to reproduce the motion of the sliding mass, considering the effects of the friction coefficient of each slip surface, and the strength of the parallel bonds and the contact stiffness of the particles on the run-out distance and deposition pattern. Six typical cross sections of the deposition mass were compared with field measurements to determine the best-fit microscopic parameters for the numerical simulation. The dynamic process of the landslide was studied by simulating the position and velocity of each particle during the movement of the sliding mass.

The friction coefficient had the strongest effect on the run-out distance and deposition pattern of the sliding mass compared with the parallel bond strength and contact. Based on comparison of the simulation results and field measurements, best-fit microscopic parameters for the numerical reproduction of the Wenjiagou landslide are a surface friction

coefficient of 0.2, parallel bond strength of 2 MPa, and contact stiffness of  $2 \times 10^8$  kN/m. The model showed that the Wenjiagou landslide lasted about 115 s from the initial movement to the final deposition of all the particles. Because of the three strong collisions with the valley slopes along the sliding path, most of the debris mass was deposited in the valley, and the velocity reached a maximum of 114 m/s.

This study shows that the dynamic mechanism and deposition process of a rock landslide can be well simulated. Using a numerical model based on the discrete element method, the velocity of the sliding mass, the deposition area, influence extent, and degree of damage to structures resulting from the sliding event can be assessed for other potential landslide sites.

**Acknowledgements** This study was supported by the National Natural Science Foundation of China (No. U1704243), Key Scientific Research Project Plan of Henan Higher Education Institutions (No. 17A410002), Project of Levee Safety and Disease Control Engineering Technology Research Center of The Ministry of Water Resources of the People's Republic of China, and The Project of High Level Talents in North China University of Water Resource and Electric Power (No. 201518). We thank Dalia Lahav-Jones, from Liwen Bianji, Edanz Group China ([www.liwenbianji.cn/ac](http://www.liwenbianji.cn/ac)), for editing the English text of a draft of this manuscript.

## References

- Capra L, Sulpizio R, Márquez-Ramírez VH, Coviello V, Doronzo DM, Arambula-Mendoza R, Cruz S (2018) The anatomy of a pyroclastic density current: the 10 July 2015 event at Volcán de Colima (Mexico). *Bull Volcanol* 80:34. <https://doi.org/10.1007/s00445-018-1206-4>
- Chen G, Zhao Q, Huang H (2011) Sliding characteristics of high-speed and long run-out giant rockslide landslide at Wenjiagou stream. *J Eng Geol* 19(03):404–408

- Clague J, Souther J (1982) The Dusty Creek landslide on mount Cayley, British Columbia. *Can J Earth Sci* 19(3):524–539
- Cundall PA, Strack ODL (1979) A discrete numerical model for granular assemblies. *Géotechnique* 30(30):331–336
- Evans SG, Hungr O, Clague JJ (2001) Dynamics of the 1984 rock avalanche and associated distal debris flow on mount Cayley, British Columbia, Canada; implications for landslide hazard assessment on dissected volcanoes. *Eng Geol* 61(1):29–51
- Giani GP (1992) Rock slope stability analysis. A. A. Balkema, Rotterdam, p 361
- Hoek E, Brown ET (1997) Practical estimates of rock mass strength. *Int J Rock Mech Min Sci* 34:1165–1186. [https://doi.org/10.1016/S1365-1609\(97\)80069-X](https://doi.org/10.1016/S1365-1609(97)80069-X)
- Huang H (2010) Preliminary study on the mechanism and kinematics characteristics of rockslides (Sturzstrom) triggered by earthquake. Dissertation. Chengdu University of Technology
- Huang R, Pei X, Li T (2008) Basic characteristics and formation mechanism of the largest scale landslide at Daguangbao occurred during the Wenchuan earthquake. *J Eng Geol* 16(06):730–741
- Jiang X (2011) Three dimensional discrete element simulation of landslide process of Wenjiagou Mianzhu. Dissertation. China University of Geosciences (Beijing)
- Larson MK, Iverson SR, Stewart BM, Walker K (1998) Preliminary assessment of particle flow code as a tool to assess ore pass safety. *Int J Rock Mech Min Sci* 35(4):533–533
- Liang Y (2014) Study on Wenjiagou landslide characteristics based on remote sensing image. Dissertation. China University of Geosciences(Beijing)
- Lin C-H, Lin M-L (2015) Evolution of the large landslide induced by typhoon Morakot: a case study in the Butangbunasi River, southern Taiwan using the discrete element method. *Eng Geol* 197:172–187. <https://doi.org/10.1016/j.enggeo.2015.08.022>
- Lo CM, Lin ML, Tang CL, Hu JC (2011) A kinematic model of the Hsiaolin landslide calibrated to the morphology of the landslide deposit. *Eng Geol* 123(1–2):22–39
- Lu CY, Tang CL, Chan YC, Hu JC, Chi CC (2014) Forecasting landslide hazard by the 3D discrete element method: a case study of the unstable slope in the Lushan hot spring district, Central Taiwan. *Eng Geol* 183:14–30
- Lube G, Cronin SJ, Platz T, Freundt A, Procter JN, Henderson C (2007) Flow and deposition of pyroclastic granular flows: a type example from the 1975 Ngauruhoe eruption, New Zealand. *J Volcanol Geotherm Res* 161(3):165–186
- Orwin JF, Clague JJ, Gerath RF (2004) The Cheam rock avalanche, Fraser Valley, British Columbia, Canada. *Landslides* 1(4):289–298
- Patra AK et al (2005) Parallel adaptive numerical simulation of dry avalanches over natural terrain. *J Volcanol Geotherm Res* 139:1–21. <https://doi.org/10.1016/j.jvolgeores.2004.06.014>
- Potyondy DO, Cundall PA (2004) A bonded-particle model for rock. *Int J Rock Mech Min Sci* 41(8):1329–1364
- Shaller PJ (1991) Analysis of a large moist landslide, Lost River Range, Idaho, USA. *Can Geotech J* 28(4):584–600
- Shi F (2014). The study of rapid and long-runout characteristics of Wenjiagou landslide based on PFC3D. Dissertation. China University of Geosciences (Beijing)
- Su O, Akcin NA (2011) Numerical simulation of rock cutting using the discrete element method. *Int J Rock Mech Min Sci* 48(3):434–442
- Su S, Zhang Y, Li S, Hao L, Wang K, Mei H (2010) Numerical analysis on motion mechanism of high-speed and long runout landslide by Wenchuan earthquake—taking Xiejadianzi landslide as an example. *J Earth Sci Environ* 32(03):277–287
- Tang CL, Hu JC, Lin ML, Angelier J, Lu CY, Chan YC, Chu HT (2009) The Tsaoling landslide triggered by the Chi-Chi earthquake, Taiwan: insights from a discrete element simulation. *Eng Geol* 106:1–19
- Wang T, Shi J, Wu S, Zhang Y, Li B, Xin P, Sun P (2010) Formation mechanism of Wenjiagou high speed and long run-out debris avalanche triggered by Wenchuan earthquake. *J Eng Geol* 18(05):631–644
- Wang Y, Cheng Q, Zhu Q (2012) Inverse grading analysis of deposit from rock avalanches triggered by Wenchuan earthquake. *Chin J Rock Mech Eng* 31(06):1089–1106
- Wu S, Wang T, Shi L, Sun P, Shi J, Li B, Xin P, Wang J (2010) Study on catastrophic landslides triggered by 2008 Wenhcuan earthquake, Sichuan, China. *J Eng Geol* 18(02):145–159
- Zhang M, Yin Y (2013) Dynamics, mobility-controlling factors and transport mechanisms of rapid long-runout rock avalanches in China. *Eng Geol* 167:37–58
- Zhang M, Yin Y, McSaveney M (2016) Dynamics of the 2008 earthquake-triggered Wenjiagou Creek rock avalanche, Qingping, Sichuan, China. *Eng Geol* 200:75–87